Iron distributions in the water column of the Japan Basin and Yamato Basin (Japan Sea)

Satoshi Fujita,[1] Kenshi Kuma,[1] Satoko Ishikawa,[1] Shotaroh Nishimura,[1] Yuta Nakayama,[1] Satomi Ushizaka,[1] Yutaka Isoda,[2] Shigeyoshi Otosaka,[3] and Takafumi Aramaki[4]

Received 15 January 2010; revised 28 July 2010; accepted 11 August 2010; published 1 December 2010.

[1] In the Japan and Yamato basins (Japan Sea), dissolved Fe ([D-Fe], <0.22 μm fraction) was characterized by surface depletion, mid-depth maxima, then a slight decrease with depth in deep water and uniform concentration in bottom waters because of biological uptake in the surface water and release by microbial decomposition of sinking organic matter in mid-depth waters. Total Fe concentrations ([T-Fe]) in the surface water of the Japan Sea were 1–4 nM, a little higher than those in the surface waters of the nutrient-deficient subtropical western North Pacific and extremely higher than the nutrient-rich subarctic western North Pacific and the nutrient-deficient subtropical central North Pacific, resulting from high atmospheric Fe input to nutrient-depleted surface water of the Japan Sea. In the Japan Basin, the [T-Fe] in bottom water were lower than those in deep water, resulting from (1) the injection of new bottom water with the lower [T-Fe] into the Japan Basin bottom water, (2) the particulate Fe removal by particle scavenging during the bottom water circulation of the Japan Basin, or (3) the injection of deep water with the higher [T-Fe] into the Japan Basin deep water. On the other hand, the [T-Fe] in deep water of the Yamato Basin and the slope regions were variable with different [T-Fe] levels among stations and depths. We found a significant relationship between [T-Fe] and water transmittance in deep water, probably resulting from the iron supply into the deep water because of the lateral transport of resuspended sediment from the slope.

Citation: Fujita, S., K. Kuma, S. Ishikawa, S. Nishimura, Y. Nakayama, S. Ushizaka, Y. Isoda, S. Otosaka, and T. Aramaki (2010), Iron distributions in the water column of the Japan Basin and Yamato Basin (Japan Sea), *J. Geophys. Res.*, *115*, C12001, doi:10.1029/2010JC006123.

1. Introduction

[2] The Japan Sea, which is connected to the East China Sea, the western North Pacific Ocean, and the Okhotsk Sea with shallower sills than 150 m depth, is one of the largest marginal seas in the world and is formed by the Japan, Yamato and Tsushima Basins with water depths of about 2000–3500 m (Figure 1). The deep water (the Japan Sea proper water (JSPW)) has its own deep convection within the Japan Sea and is characterized by a uniform water mass with narrow ranges of temperature (0.0–1.0°C) and salinity (34.06–34.08) below approximately 500 m depth. However, several studies have revealed that the structure of the JSPW is composed of three water layers: the upper layer (UJSPW) above about 1000 m depth, Japan Sea Deep Water (JSDW) between approximately 1000 and 2000–2500 m depths, and Japan Sea Bottom Water (JSBW) below 2000–2500 m depth [*Gamo and Horibe*, 1983; *Gamo et al.*, 1986; *Sudo*, 1986; *Senjyu et al.*, 2005a; *Kumamoto et al.*, 2008].

[3] Despite the great interest in the behavior of iron in open oceans, our understanding of the biogeochemical and physical mechanisms that regulate iron and other trace metals is still limited in marginal seas, such as the Japan Sea, the Bering Sea and the Okhotsk Sea. In general, dissolved Fe ([D-Fe]) in remote oceanic regions are characterized by surface depletion and a gradual increase with depth below the surface water and release from microbial decomposition of sinking organic matter in deep water [*Johnson et al.*, 1997]. [D-Fe] distributions in the deep water column are mainly controlled by the production of dissolved Fe from particulate organic matter (POM) during carbon remineralization [*Johnson et al.*, 1997], the particle scavenging removal dissolved Fe [*Bergquist and Boyle*, 2006; *Bergquist et al.*, 2007], and the complexation of Fe with natural organic ligands [e.g., *Kuma et al.*, 2003; *Laglera and van den Berg*, 2009; *Kitayama et al.*, 2009]. These processes would lead to mid-depth maxima and, below that, a slight decrease in the [D-Fe] with depth in deep water in the

[1]Graduate School of Environmental Science, Hokkaido University, Sapporo, Japan.
[2]Faculty of Fisheries Sciences, Hokkaido University, Hakodate, Japan.
[3]Research Group for Environmental Science, Japan Atomic Energy Agency, Naka-gun, Ibaraki, Japan.
[4]Environmental Chemistry Division, National Institute for Environmental Studies, Tsukuba, Japan.

0148-0227/10/2010JC006123

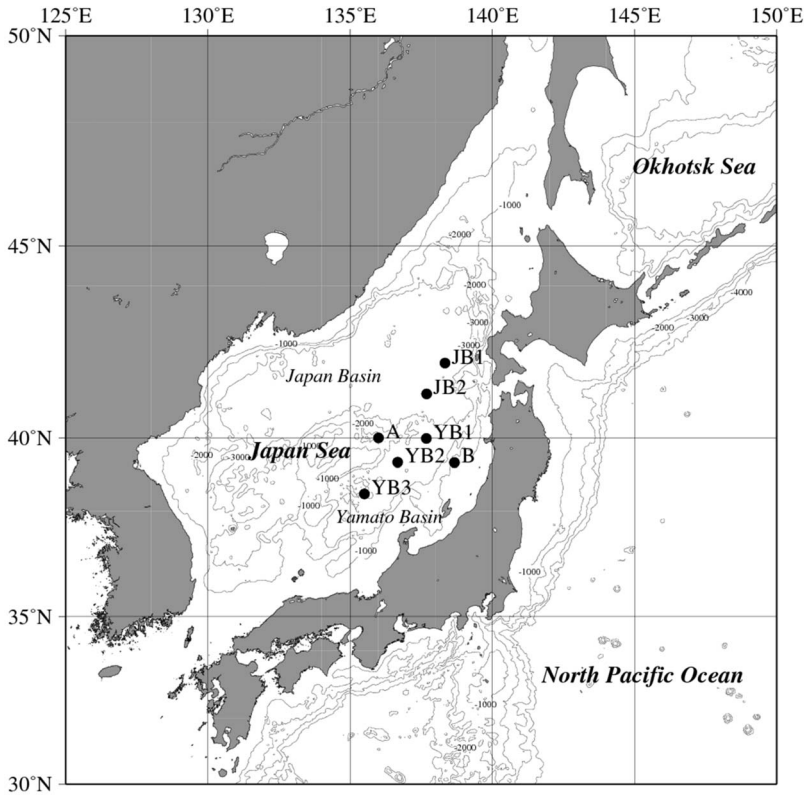

Figure 1. Locations of sampling stations in the Japan Basin (JB1 and JB2), in the Yamato Basin (YB1, YB2, and YB3) and in the slope region (Station A and Station B) in the Japan Sea during 5–9 November 2007.

North Pacific Ocean [*Martin et al.*, 1989; *Johnson et al.*, 1997; *Nakabayashi et al.*, 2001; *Nishioka et al.*, 2003, 2007; *Takata et al.*, 2006; *Kitayama et al.*, 2009]. However, particulate Fe ([P-Fe], total dissolvable Fe ([T-Fe]) minus [D-Fe]) with short residence time in deep water may be sensitive to change in the water masses and the resuspension of sediments from the seafloor or the slope in various oceanic sites [*Otosaka et al.*, 2004, 2008; *Takata et al.*, 2006, 2008; *Nishioka et al.*, 2007; *Lam and Bishop*, 2008; *Kitayama et al.*, 2009].

[4] Ecosystems in marginal seas are in close proximity to terrestrial and continental shelf sources of Fe. Iron is generally supplied to surface water by the upwelling, vertical water mixing, atmospheric and riverine inputs [*Hutchins et al.*, 1998; *Kuma et al.*, 2000; *de Baar and de Jong*, 2001; *Jickells and Spokes*, 2001; *Saitoh et al.*, 2008]. Recently, it has been reported that iron supplied from continental shelf sediments to the surface water by wind-driven upwelling induced the high productivity in central California waters [*Johnson et al.*, 1999, 2001; *Fitzwater et al.*, 2003; *Elrod et al.*, 2004, 2008; *Chase et al.*, 2005]. In addition, several studies in other regions, such as the Alaskan coast, the east coast of New Zealand and the European shelf, have also reported that lateral supply of iron from the continental margin is an important source to the open ocean [*Croot and Hunter*, 1998; *Laës et al.*, 2003, 2007; *Lam et al.*, 2006; *Lam and Bishop*, 2008; *Ussher et al.*, 2007]. However, the transport mechanisms and the magnitudes of the various sources in the iron cycles of the coastal and marginal seas are not well known. It is likely that iron is supplied to the semiclosed Japan Sea, close to the Asian continent, from the different sources, such as (1) aeolian Asian dust deposition, (2) transport of water masses and (3) vertical and lateral transport of sediments from seafloor, continental shelf and slope.

[5] Here, we report the vertical distributions of iron ([D-Fe] and [T-Fe]), and chemical and biological components [humic-type fluorescence (H-flu) intensity, nutrient, oxygen, and chlorophyll *a* (Chl-*a*) concentrations] throughout the water column in the basin (Japan Basin and Yamato Basin) and slope regions in the Japan Sea in order to understand the mechanisms that control iron behavior in the water column.

2. Methods

2.1. Sample Collections and Treatment

[6] Figure 1 shows the sampling stations in the Japan Sea. Seawater samples were collected at 5–3600 m depths at two stations (JB1 and JB2) in the eastern Japan Basin, 5–2600–2950 m depths at three stations (YB1, YB2 and YB3) in the central Yamato Basin and 5–700–1350 m depths at two stations (A and B) in the edge of Yamato Basin (slope region) in the eastern Japan Sea during 5–9 November 2007 (Table 1) using acid-cleaned, Teflon-coated, 10-L Niskin X sampling bottles (General Oceanics) attached to a CTD-RMS. Sample filtration for analyses of [D-Fe] and H-flu intensity was carried out by connecting an acid-cleaned 0.22 μm pore size Durapore membrane filter (Cartridge-type-Millipak 100 with large filtering surface area, Millipore) to a sampling bottle spigot and then filtering with gravity filtration. The filtrate (7–8 ml) for H-flu intensity analysis

Table 1. Position of Stations, Bottom Depth, and Sampling Date in the Northeastern (Japan Basin) and Eastern (Yamato Basin) Japan Sea[a]

Station	Position		Bottom Depth (m)	Sampling Date
	Latitude (N)	Longitude (E)		
(Japan Basin Region)				
JB1	42°00.0′	138°20.0′	3683	5 Nov 2007
JB2	41°11.1′	137°41.1′	3678	6 Nov 2007
(Yamato Basin Region)				
YB1	39°59.3′	137°41.0′	2700	7 Nov 2007
YB2	39°20.5′	136°40.5′	2656	8 Nov 2007
YB3	38°28.3′	135°29.9′	3002	9 Nov 2007
(Slope in Yamato Basin Region)				
A	40°00.1′	136°00.0′	1428	6 Nov 2007
B	39°20.0′	138°40.0′	721	7 Nov 2007

[a]See Figure 1.

was immediately frozen in 10 ml acrylics tubes to <−20°C in the dark until measurement in the laboratory. The freezing treatment was used to prevent the possible microbial degradation of natural humic-type fluorescent dissolve organic matter (humic-type FDOM) in the filtered seawater. Unfiltered samples were collected for [T-Fe], Chl-*a* and nutrient concentrations. The filtered and unfiltered seawater (100 ml in precleaned 125 ml low-density polyethylene (LDPE) bottles) used for [D-Fe] (<0.22 μm fraction) and [T-Fe] (unfiltered) analyses were acidified with ultrapure grade HCl to pH 1.7–1.8 in a class 100 clean-air bench on board after collection. The acidified iron samples (pH 1.7–1.8) were allowed to stand at room temperature for three months at least until iron analysis in the laboratory [*Bruland and Rue*, 2001; *Lohan et al.*, 2005].

[7] Hydrographic observations (salinity, temperature, depth and dissolved oxygen (DO) concentration) were conducted with a CTD (Conductivity Temperature Depth probe and DO sensor).

2.2. Dissolved and Total Dissolvable Fe Concentrations

[8] The acidified iron samples were buffered at pH 3.2 with a 8.15 M formic acid −4.4 M ammonium buffer solution (0.8 ml per 100 ml sample solution) in a class 100 clean-air bench in the laboratory. The iron concentrations ([D-Fe] and [T-Fe]) in buffered 0.22 μm filtered and unfiltered samples were determined by an automated Fe analyzer (Kimoto Electric Co. Ltd.) by use of a combination of chelating resin concentration and luminol-hydrogen peroxide chemiluminescence (CL) detection in a closed flow through system [*Obata et al.*, 1993] as reported in our previous studies [*Nakabayashi et al.*, 2001; *Takata et al.*, 2004, 2005, 2006, 2008; *Kitayama et al.*, 2009]. Briefly, iron in a buffered sample solution was selectively collected on 8-hydroxyquinoline immobilized chelating resin and then eluted with dilute 0.3 N HCl. The eluent was mixed with luminol solution, 0.6 N aqueous ammonia and 0.7 M H_2O_2 solution successively, and then the mixture was introduced into the CL cell. Finally, the iron concentration was determined from the CL intensity. Accuracy of this analysis was checked using the SAFe reference materials (pH 1.7–1.8). The SAFe reference materials were found to be within the range of the consensus values of 0.097 ± 0.043 nM for S1 and 0.91 ± 0.17 nM for D2 [*Johnson*, 2007] (GEOTRACES homepage, www.geotraces.org). The [D-Fe] of S1 and D2 reference samples, which were determined by our analytical method after being buffered at pH 3.2 in the present study, were 0.113 ± 0.004 nM and 0.99 ± 0.09 nM within the range of the consensus values, respectively.

[9] In our previous studies, there were no differences in the [D-Fe] of directly buffered 0.22 μm-filtered oceanic samples to pH 3.2 (without acidification of seawater samples to pH 1.7–1.8 in the present study) that had been kept for one month and six months (for example, 0.28 and 0.27 nM at 50 m depth and 1.10 and 1.09 nM at 200 m depth, respectively, at an oceanic station in the northwestern North Pacific Ocean [*Takata et al.*, 2004]). However, it is unclear what the effect of weak acidification to pH 3.2 would have on solubilizing any colloidal Fe phases that might be present in the "dissolved" fraction ([D-Fe], <0.22 μm fraction), an uncertainty of great concern especially in estuarine and coastal waters, where dissolved Fe concentrations may be higher and colloidal Fe comprises a greater fraction [*Bruland and Rue*, 2001]. In addition, the weak acidification of unfiltered seawater samples may lead to measure some operational fraction of the acid leachable particulate Fe and dissolved Fe fraction. Therefore, the filtered and unfiltered seawater used for [D-Fe] and [T-Fe] analyses in the present study were acidified with ultrapure HCl to pH 1.7–1.8 on board as soon as the samples were collected and then kept at room temperature for 3 months at least until iron analysis in the laboratory.

2.3. Humic-Type FDOM, Nutrient, Dissolved Oxygen, Chl-*a* Concentrations and Water Transmittance

[10] The frozen 0.22 μm-filtered samples in acrylics tubes were thawed and warmed overnight to room temperature in the dark, the humic-type FDOM was measured as the H-flu intensity in a 1 cm quartz cell with a Hitachi F-2000 fluorescence spectrophotometer at 320 nm excitation and 420 nm emission, using 10 nm bandwidths [*Hayase et al.*, 1988; *Hayase and Shinozuka*, 1995] as reported in previous studies [*Tani et al.*, 2003; *Takata et al.*, 2004, 2005; *Kitayama et al.*, 2009]. Fluorescent intensity was expressed in terms of quinine sulfate units (1 QSU = 1 ppb quinine sulfate in 0.05 M H_2SO_4, excitation 320 nm, emission 420 nm [*Mopper and Schultz*, 1993]). Major nutrient [phosphate (PO_4), nitrate plus nitrite (NO_3+NO_2), and silicate (SiO_2)] concentrations were determined using a Technicon autoanalyzer. Dissolved oxygen (O_2measured) was determined on board by the Winkler titration method with potentiometer end point using a 798 MPT Titrino analyzer (Metrohm). The apparent oxygen utilization (AOU) was calculated by subtracting the measured oxygen content (O_2measured) from the saturation value (O_2sat) of the dissolved oxygen [*Hansen*, 1999]. The concentrations of Chl-*a* were determined by the fluorometric method after extraction with N, N-dimethylformamide [*Suzuki and Ishimaru*, 1990]. The beam transmittance (%) in the water column was measured using single-channel transmissometer (path length: 25 cm; wavelength: 470 nm; bandwidth: ~20 nm, WET Labs, Inc.) with relationship of transmittance (Tr) to beam attenuation coefficient (c), and path length (x): $Tr = e^{-cx}$. In the present study, the vertical profiles of water transmittance [Tr (%)] in the water column were consistent with those of the turbidity [*Takata et al.*, 2008] although suspended particles, phytoplankton, bacteria

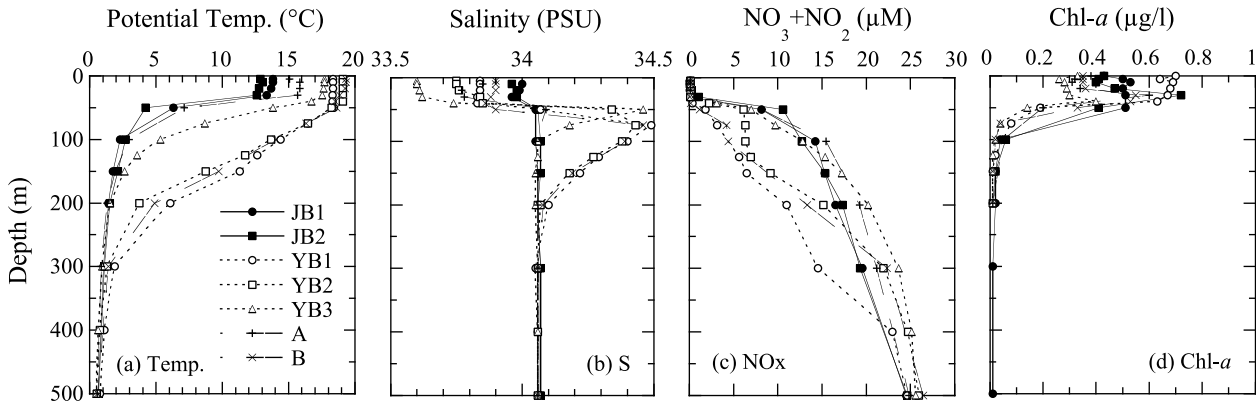

Figure 2. Vertical distributions of (a) potential temperature, (b) salinity, (c) NO_3+NO_2, and (d) Chl-*a* at the surface water upper 500 m depth in the Japan Sea.

and dissolved organic matter all contribute to the losses sensed by the instrument.

3. Results

3.1. Iron and Physical and Biochemical Components in the Surface Water

[11] In the surface mixed layer (<40 m depth), potential temperature (12–14°C) at JB1 and JB2 in the Japan Basin were relatively lower than those (15–19°C) at YB1, YB2 and YB3 in the Yamato Basin and at Station A and Station B in the slope region, while salinity (33.97–34.0) at JB1 and JB2 were relatively higher than those (33.60–33.90) at YB1, YB2, YB3 and at Station A and Station B (Figures 1, 2a, and 2b). In the surface mixed layer at all stations, extremely low nutrient concentrations [0.1–0.2 μM for NO_3+NO_2 (Figure 2c), 0.04–0.14 μM for PO_4, and 2.2–4.7 μM for SiO_2] and relatively low Chl-*a* concentrations (0.3–0.7 μg/l, Figure 2d) were observed, while [D-Fe] and [T-Fe] levels were high with the ranges of 0.33–2.04 nM and 0.85–6.57 nM, respectively (Figures 3, 4, and 5).

[12] At YB1 and YB2 in the Yamato Basin and Station B in the slope region, potential temperature tended to decrease gradually just below the surface mixed layer, while salinity increase to a maximum (34.4–34.5) just below the surface mixed layer and then decrease gradually with depth to 34.06–34.07 at 300 m depth. On the contrary, rapid decreases in potential temperature and relatively constant salinity (34.05–34.07) below the surface mixed layer were observed at JB1 and JB2 in the Japan Basin, YB3 in the Yamato Basin and Station A in the slope region (Figures 2a and 2b). The nutrient concentrations below the surface mixed layer tended to increase gradually with depth at YB1, YB2 and Station B and to increase rapidly with depth at JB1, JB2, YB3 and Station A (Figure 2c). The increasing tendency of nutrients below the surface mixed layer is remarkably similar to the decreasing tendency of potential temperature (Figures 2a and 2c). The [D-Fe] in the surface water below the surface mixed layer tended to increase gradually from ~0.7–1 nM to ~1.7–2.3 nM with depth at all stations (Figures 3, 4, and 5). However, there are two types of [T-Fe] profiles in the surface waters below the surface mixed layer: (1) gradual increase with depth to ~5–8 nM at 500 m depth

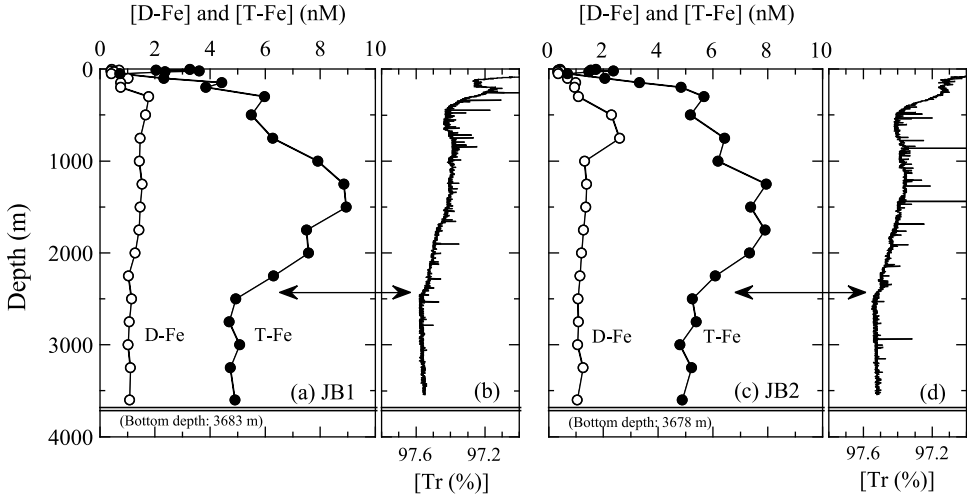

Figure 3. Vertical distributions of dissolved Fe concentration ([D-Fe], open circle), total Fe concentration ([T-Fe], solid circle) and water transmittance [Tr (%)] in (a and b) JB1 and (c and d) JB2. The spikes in [Tr (%)] were due to ambient noise.

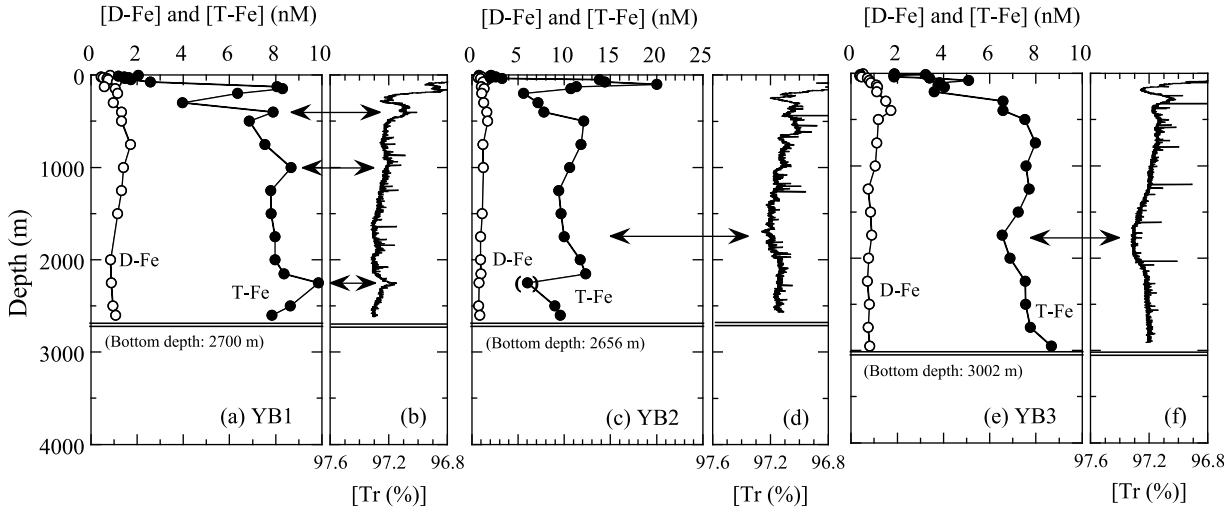

Figure 4. Vertical distributions of dissolved Fe concentration ([D-Fe], open circle), total Fe concentration ([T-Fe], solid circle) and water transmittance [Tr (%)] in (a and b) YB1, (c and d) YB2, and (e and f) YB3. The spikes in [Tr (%)] were due to ambient noise.

for JB1, JB2, YB3 and Station A (Figures 3a, 3c, 4e, and 5a) and (2) maximum concentrations (8.3 nM, 20 nM and 33 nM at YB1, YB2 and Station B, respectively) at the depth range of 100–150 m (Figures 4a, 4c, and 5c).

3.2. Iron and Physical and Biochemical Components in the Deep Water Column

[13] Potential temperature rapidly decreases below the surface mixed layer in both basins (Figure 2a) and is almost homogenous with narrow range of 0.0–0.8°C below 500 m depth. In addition, Sigma-θ, salinity and DO concentration below approximately 1000 m depth in both basins were almost homogenous with narrow ranges of 27.33–27.35, 34.06–34.07 and 4.5–4.7 ml/l, respectively (Figures 6a, 6b, and 6c for the Japan Basin). NO_3+NO_2 concentration and H-flu intensity in the Japan Sea were characterized by surface depletion, gradual increase with depth in mid-depth water (upper 1000 m depth) and remarkably uniform values (25.9–27.5 μM for NO_3+NO_2 and 2.8–3.6 QSU for H-flu intensity) in deep and bottom waters below 1000 m depth (Figures 6d and 6e).

[14] The [D-Fe] was generally low at the surface (0.3–1 nM upper 200 m depth), high with the maximum values (1.7–2.6 nM in the Japan and Yamato Basins) at the depth range of 300–750 m, then a slight decrease with depth in deep water, and with uniform in bottom water (approximately 1.0–1.1 nM below 2250 m depth in the Japan Basin and approximately 0.7–1.0 nM below 2000 m depth) (Figures 3, 4, and 5). The depth profiles of [T-Fe] in both basins and slope regions were remarkably different from those of [D-Fe], DO, nutrients and H-flu intensity (Figures 3, 4, 5, and 6). The [T-Fe] in the deep-water column of the Japan

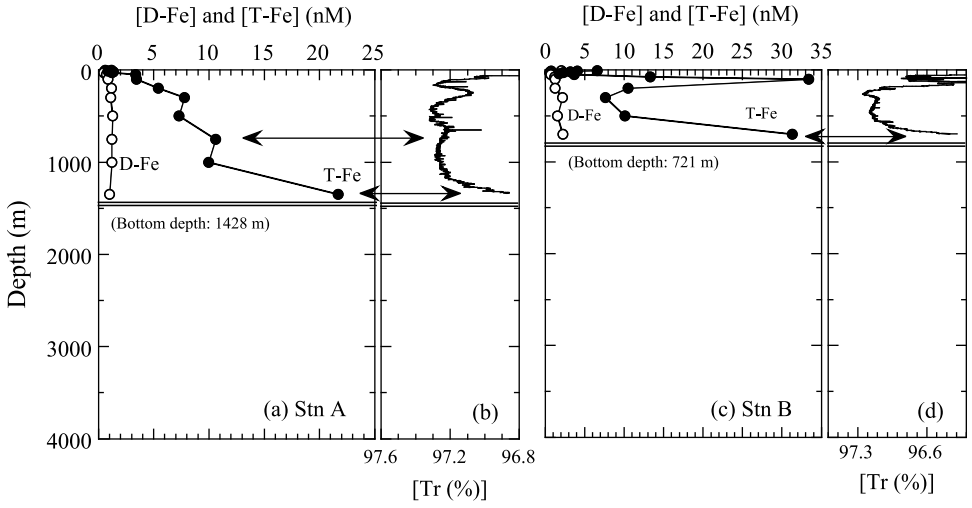

Figure 5. Vertical distributions of dissolved Fe concentration ([D-Fe], open circle), total Fe concentration ([T-Fe], solid circle) and water transmittance [Tr (%)] in the slope region (a and b) Station A and (c and d) Station B around the Yamato Basin. The spikes in [Tr(%)] were due to ambient noise.

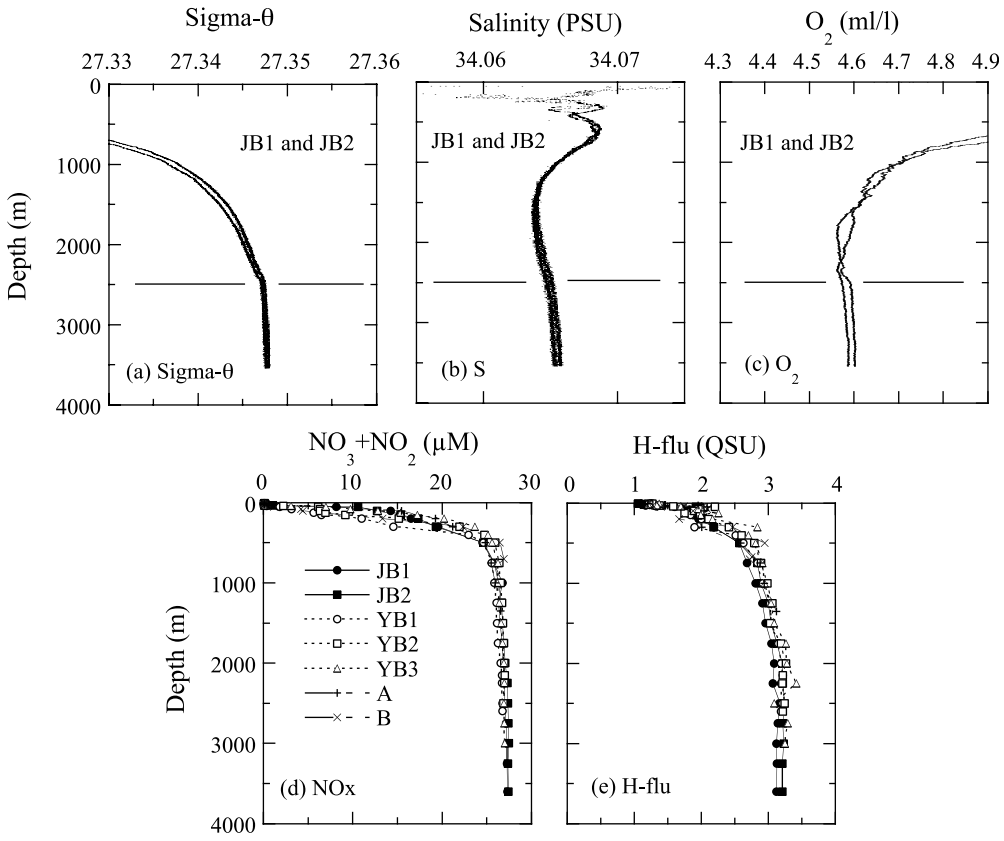

Figure 6. Vertical distributions of (a) sigma-θ, (b) salinity, and (c) DO in the water column of the Japan Basin (JB1 and JB2) and (d) NO_3+NO_2 and (e) H-flu intensity in the water column of the Japan Basin (JB1 and JB2), Yamato Basin (YB1, YB2, and YB3) and slope region (Station A and Station B) in the Japan Sea.

Basin (JB1 and JB2) rapidly increased with depth to 8–9 nM at the depth of 1250–1500 m, then decreased with depth to 5 nM at the depth of 2500 m and relatively uniform with approximately 5 nM below 2500 m depth (Figure 3). Those of the Yamato Basin (YB1, YB2 and YB3) are variable with different depth profiles and levels of [T-Fe] among stations (7–10 nM at YB1, 8–12 nM at YB2 and 6–9 nM at YB3, Figure 4). In addition, those of the slope regions (Figure 5) rapidly increased with depth to 21.7 nM at 1350 m depth near bottom (Station A: bottom depth of 1428 m) and to 31.3 nM at 700 m depth near bottom (Station B: bottom depth of 721 m). Below 500 m depth, the depth profiles of [T-Fe] in the deep water column of all stations are remarkably similar to those of water transmittance with higher [T-Fe] at lower transmittance (Figures 3, 4, and 5).

4. Discussion

4.1. Iron and Biological and Chemical Components in the Surface Water

[15] The [D-Fe] and [T-Fe] levels throughout the water column in the Japan and Yamato Basins in the present study were approximately 2 times higher than those in a previous study [*Takata et al.*, 2008]. Therefore, the strong acidification of filtered and unfiltered seawater samples to pH 1.7–1.8 in the present study (pH 3.2 in the previous study) is necessary to solubilize any colloidal Fe phases that might be present in the [D-Fe] (filtered) and [T-Fe] (unfiltered) fractions, especially in estuarine, coastal and marginal waters, where dissolved Fe concentrations may be higher and colloidal Fe comprises a greater fraction [*Bergquist and Boyle*, 2006; *Bergquist et al.*, 2007; *Bruland and Rue*, 2001].

[16] The Tsushima Warm Current (TWC) passing into the Japan Sea through the Tsushima Strait flows along the northwestern Japanese coast in the northeastern Japan Sea. TWC carries both the subtropical water originating from the Kuroshio Current in the North Pacific and the runoff water from the continental shelf in the East China Sea to the Japan Sea [*Isobe et al.*, 2002]. At all stations (YB1, YB2 and YB3) in the Yamato Basin and at Station B in the slope region, the surface high temperature (17–20°C) and low salinity (33.6–33.9) occurred in the surface mixed layer upper 40 m depth, and the subsurface high-salinity water (>34.1) occurred from 50 m to 100–200 m depths with a maximum salinity (34.4–34.5 at 50–75 m depth) just below the surface mixed layer (Figures 1, 2a, and 2b). The surface mixed layer with high temperature and low salinity is the upper portion of the TWC water originating from the continental shelf and the subsurface water with high salinity is the lower portion of the TWC water originating from the North Pacific [*Watanabe et al.*, 2006]. In the surface mixed layer, extremely low nutrient, low Chl-*a* and remarkably high Fe concentrations ([D-Fe] = ~0.3–2 nM and [T-Fe] = ~1–7 nM) were observed at the depth range of 5–40 m (Figures 3, 4, and 5). Therefore,

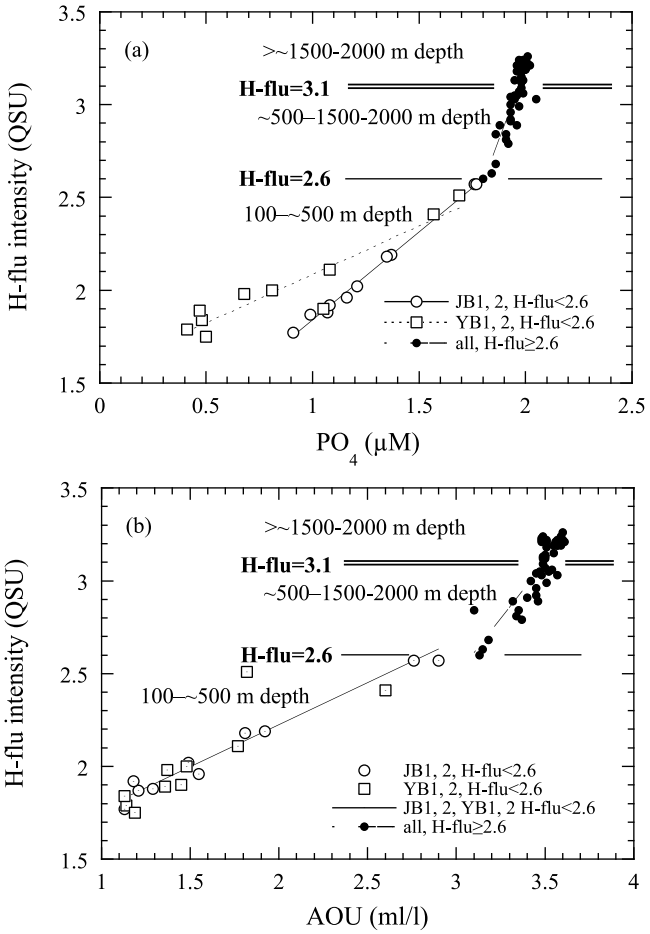

Figure 7. H-flu intensity versus (a) PO_4 concentration and (b) apparent oxygen utilization in the deep water column (≥100 m depth) of the Japan Basin (JB1 and JB2) and the Yamato Basin (YB1 and YB2).

phytoplankton growth in the surface mixed layer in the Japan Sea, which was characterized by low nutrient and high Fe concentrations, could be limited by macronutrient deficiency. The high Fe concentrations in the surface mixed layer probably result from the high atmospheric Fe input to nutrient-depleted surface water of the Japan Sea close to the Asian continent [*Duce and Tindale*, 1991; *Jickells and Spokes*, 2001; *Jo et al.*, 2007; *Obata et al.*, 2007]. In our previous study [*Kitayama et al.*, 2009], we observed relatively high [D-Fe] and [T-Fe] in the surface mixed layer with extremely low nutrient concentrations at the western subtropical North Pacific station, probably resulting from higher atmospheric Fe input than biological Fe uptake in the oligotrophic surface mixed layer.

[17] At YB1 and YB2 in the Yamato Basin and at Station B in the slope region of the western Japan, the gradually decreasing potential temperature and the gradually increasing nutrient concentrations with depth and high salinity (>34.07) below the surface mixed layer (Figures 2a, 2b, and 2c) are due to the inflow of the lower portion of the TWC water with high temperature, high salinity and low nutrient flowing along the northwestern Japanese coast in the eastern Japan Sea. The lower portion of the TWC water originates from the Kuroshio Current with high temperature, high salinity and low nutrient passing into the Japan Sea through the Tsushima Strait [*Hase et al.*, 1999; *Watanabe et al.*, 2006]. Furthermore, the relationship between H-flu intensity and PO_4 concentrations at 100–~500 m depth range is apparent that the slope in the YB1 and YB2 is lower than that in the JB1 and JB2 with the increase in H-flu intensity with depth in association with the increase in PO_4 concentrations (Figure 7a), probably resulting from the inflow of the lower portion of the TWC water into the YB1 and YB2. However, the deep and bottom waters and the relationship between H-flu intensity and AOU in the water column (Figure 7b) do not show this trend between H-flu intensity and PO_4 concentrations at 100–~500 m depth range.

[18] The maximum [T-Fe] in the surface water were observed in the narrow depth range of 100–150 m at YB1, YB2 and Station B (8.3 nM, 20 nM and 33 nM at YB1, YB2 and Station B, respectively, Figures 4a, 4c, and 5c) where the subsurface water is characterized by the lower portion of the TWC. In addition, the vertically integrated [T-Fe] (particulate Fe concentration ([P-Fe]) plus [D-Fe]) inventories in the upper 200 m (5–200 m interval) at YB1, YB2 and Station B were remarkably high with 958, 2,024 and 3,128 μmol Fe m^{-2}, respectively (Figure 8), probably because of the subsurface supply of iron remobilized and/or resuspended from the continental shelf sediments [*de Baar and de Jong*, 2001; *Ussher et al.*, 2007; *Lam and Bishop*, 2008] to the TWC flowing along the western Japanese coast. On the other hand, the [T-Fe] below the surface mixed layer at JB1 and JB2 in the Japan Basin and at YB3 and Station A (slope region of the Yamato Rise) in the Yamato Basin increased with depth, similar to the increasing nutrient concentrations with depth (Figures 2c, 3a, 3c, 4e, and 5a). The [T-Fe] inventories in the upper 200 m ranged 475–555 μmol Fe m^{-2} at JB1 and JB2 and 690–703 μmol Fe m^{-2} at YB3 and Station A (Figure 8). These levels were approximately 2 times higher than those (284–359 μmol Fe m^{-2}) in the Japan and Yamato Basins in a previous study

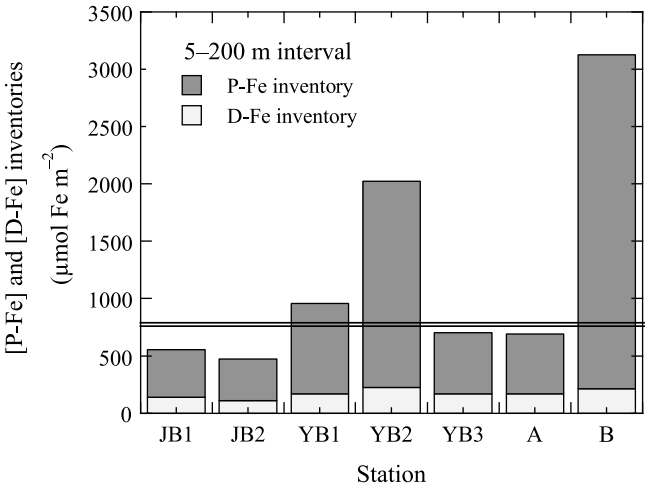

Figure 8. Vertically integrated [P-Fe] and [D-Fe] ([T-Fe] = [P-Fe]+[D-Fe]) inventories in the upper 200 m (5–200 m) of the Japan Basin (JB1 and JB2), Yamato Basin (YB1, YB2, and YB3), and slope region (Station A and Station B) in the Japan Sea.

[*Takata et al.*, 2008], because of the solubilizing colloidal Fe phases, which might be present in the [D-Fe] (filtered) and [T-Fe] (unfiltered) fractions, by the strong acidification (pH 1.7–1.8) of the filtered and unfiltered seawater used for [D-Fe] and [T-Fe] analyses in the present study. The [T-Fe] inventory levels at JB1 and JB2 were approximately 2.5–7 and 9–13 times higher than those in the western and central midlatitude oceanic regions of the North Pacific in previous study [*Takata et al.*, 2006]. The high inventory levels ranged 475–703 μmol Fe m^{-2} at JB1, JB2, YB3 and Station A in the present study were remarkably consistent with those (400–700 μmol Fe m^{-2}) at stations (17–35°W, 10–11°N) with high estimated aerosol Fe flux (~10–75 μmol Fe m^{-2} d^{-1}) close to the African coast, where are strongly influenced by atmospheric deposition from Sahara dust events [*Croot et al.*, 2004]. The high levels probably result from high atmospheric Fe input, which is originated from the Asian dust, to the surface water of the Japan Sea close to the Asian continent. In addition, [D-Fe] inventories (Figure 8) were about 23.6–25.4% (at JB1, JB2, YB3 and Station A) and 6.8–17.7% (at YB1, YB2 and Station B) of [T-Fe] present and lower than those (48 ± 10%) in the North Pacific, probably indicating the higher dust flux in the Japan Sea than the midlatitude oceanic North Pacific.

[19] There have been a variety of estimates of dust deposition to the oceans. The aerosol flux estimates are likely to be of order a factor of 10, because of uncertainties in sources, deposition, dust distribution as well as uncertainties because of the high temporal and spatial variability in dust [*Mahowald et al.*, 2005]. The highest dust concentrations are generally found in the midlatitudes and high latitudes of the North Pacific where the seasonal transport of dust from Asian desert and loess regions results in high concentrations in spring, moderate concentrations in fall, and low values in summer and winter [*Duce and Tindale*, 1991]. In our previous studies [*Takata et al.*, 2006; *Kitayama et al.*, 2009], we have estimated residence times for [T-Fe] in the western and central North Pacific by dividing the [T-Fe] inventories in the upper 200 m by the aerosol Fe flux estimates (approximately 5 and 0.5 μmol Fe m^{-2} d^{-1} as each annual average value in the western and central North Pacific, respectively [*Duce and Tindale*, 1991; *Fung et al.*, 2000]). In same manner, we estimated residence times for [T-Fe] in the Japan Sea from the [T-Fe] inventories in the upper 200 m at JB1, JB2, YB3 and Station A and the aerosol Fe flux estimate in the Japan Sea (approximately 50 μmol Fe m^{-2} d^{-1} as an annual average value [*Duce and Tindale*, 1991; *Fung et al.*, 2000]). In the present study, we assumed no impact of lateral Fe input from the margins of the Japan Sea to the surface waters at JB1, JB2, YB3 and Station A because the upper 200 m at these stations is not presumably influenced from the TWC water flowing along the western Japanese coast (Figure 2). The residence times for [T-Fe] in the Japan Sea were remarkably short ranging from 9.5 to 14 d, similar to estimates ranging 2 to 12 d with the shortest times associated with high dust flux found close to the African coast [*Croot et al.*, 2004], probably indicating the high dust flux in the Japan Sea. Moreover, the residence times for [T-Fe] in the Japan Sea were shorter than 15–42 d in the western and 48–106 d in the central North Pacific Oceans in our previous studies [*Takata et al.*, 2006; *Kitayama et al.*, 2009]. In the present study, the [T-Fe] inventories in the upper 200 m and the estimated residence times for [T-Fe] in the Japan Sea were quantitatively consistent with those in the oceanic environment with high dust flux [*Croot et al.*, 2004], suggesting the best assumption for the aerosol Fe flux estimate in the Japan Sea (approximately 50 μmol Fe m^{-2} d^{-1} as an annual average value [*Duce and Tindale*, 1991; *Fung et al.*, 2000]) although the annual value may have a large seasonal variation. It has been reported that the annual total deposition flux of mineral dust measured at Sapporo in Hokkaido, northern Japan was 5.2 g m^{-2} yr^{-1} with high in spring, moderate in fall, and low values in summer and winter [*Uematsu et al.*, 2003]. The annual average deposition flux, 14 mg m^{-2} d^{-1}, was nearly consistent with the average value in fall season when we collected water samples in the Japan Sea.

[20] In addition, we estimated residence times for [D-Fe] in the surface water at JB1 and JB2 by dividing these inventories in the upper 50 m and 200 m by an estimate of Fe solubility (approximately 1.2–2.2% as an iron solubility of the Asian mineral dust sampled at Hokkaido, northern Japan [*Ooki et al.*, 2009]) for aerosol Fe flux (~50 μmol Fe m^{-2} d^{-1} as an annual average value in the Japan Sea [*Duce and Tindale*, 1991; *Fung et al.*, 2000]). The residence times were relatively long ranging 15–37 d in the upper 50 m, probably resulting from the high atmospheric Fe input to nutrient-depleted surface mixed layer with low biological Fe uptake (Figures 2c and 2d), and 120–235 d in the upper 200 m, similar to estimates (214–291 d) for the Sargasso Sea [*Jickells*, 1999]. The surface water in regions of high deposition is essentially saturated with respect to truly [D-Fe] and the principal factor affecting [D-Fe] is the rate of transformation into particulate material via biological and abiotic processes [*Johnson et al.*, 1997].

[21] We can also estimate the vertical supply of [T-Fe] to the surface mixed layer from vertical diffusivity. Estimates for vertical eddy diffusivity range from ~1–10 m^2 d^{-1} [*Talley*, 1995]. Assuming a middle range vertical diffusivity of 5 m^2 d^{-1} and a gradient of 20 nmol [T-Fe] m^{-4} between 50 and 300 m at both JB1 and JB2 (Figures 3a and 3c), we estimate a vertical mixing supply of 0.1 μmol [T-Fe] m^{-2} d^{-1} [*Martin and Gordon*, 1988; *Croot et al.*, 2007; *Lam and Bishop*, 2008]. The resulting flux estimates for the supply of Fe from below into the mixed layer are more representative of the longer-term supply of Fe in the absence of atmospheric deposition, upwelling and the possible entrainment of coastal water to this site. The estimated vertical diffusive Fe flux is significantly lower than the estimated aerosol Fe flux in the Japan Sea.

4.2. Iron and Chemical Components in the Deepwater Column

[22] Remarkably homogenous sigma-θ and salinity below 1000 m depth (Figures 6a and 6b) are referred to the Japan Sea proper water (JSPW). However, the JSPW consists of more than one water mass: UJSPW above about 1000 m depth [*Sudo*, 1986; *Senjyu and Sudo*, 1993, 1994], JSDW between about 1000 and 2000–2500 m depths and JSBW below about 2000–2500 m depth [*Gamo and Horibe*, 1983]. Uniform distributions of DO, nutrient and H-flu intensity in the deep water column of the Japan Sea (Figures 6c, 6d, and 6e) would be mainly regulated by the remineralization process of biogenic organic matter in mid-depth water. In the North Pacific, AOU, nutrients and H-flu intensity are

generally low at the surface, high from 1000 m to 2000 m, and decrease gradually with depth in the lower column below 2000 m depth, resulting from the transport of the Circumpolar Deep Water (CDW) with low AOU, nutrients and H-flu intensity, a mixture of Atlantic Bottom water and North Atlantic Deep water, into the deep and bottom waters of the North Pacific [*Hayase et al.*, 1988; *Yamashita et al.*, 2007; *Yamashita and Tanoue*, 2008; *Kitayama et al.*, 2009]. The uniform distributions of DO, nutrients and H-flu intensity in the deep water column of the semiclosed Japan Sea attribute to no dominant injection of different water mass into the deep and bottom waters.

[23] The [D-Fe] and [T-Fe] levels in the deepwater column of the Japan and Yamato Basins in the present study (Figures 3 and 4) were also approximately 1.5–2 times higher than those in previous study [*Takata et al.*, 2008], because of the solubilizing colloidal Fe phases by the stronger acidification (pH 1.7–1.8) in the present study than previous study (pH 3.2). The vertical distributions of [D-Fe] with surface depletion, mid-depth maxima and then slight decrease in deep water in the present study (Figures 3, 4, and 5) were very similar to those in the Japan Sea and the eastern North Pacific Ocean in previous studies [*Takata et al.*, 2006, 2008]. The Fe released from microbial decomposition of sinking biogenic organic matter is the primary source for [D-Fe] in deep waters, and particle scavenging is the major Fe removal pathway [*Johnson et al.*, 1997; *Bergquist and Boyle*, 2006; *Bergquist et al.*, 2007]. It is simply assumed that there is a competition between [D-Fe] input from the decomposition of biogenic organic matter and [D-Fe] removal in deep sea by particle scavenging. Therefore, the depth profiles of [D-Fe] with mid-depth maxima and then a slight decrease in deep water in the Japan Sea would be mainly regulated by the balance of these two main processes and iron complexation with natural organic ligands controlling the Fe(III) hydroxide solubility [*Kuma et al.*, 1996, 2003; *Johnson et al.*, 1997; *Takata et al.*, 2005; *Kitayama et al.*, 2009; *Schlosser and Croot*, 2009]. The depth profiles of [D-Fe] are different from those of DO, nutrient and H-flu intensity with gradual increase with depth in mid-depth water (upper 500–1000 m depth) and remarkably uniform values below 1000 m depth (Figure 6), which would be regulated by the remineralization process of biogenic organic matter in mid-depth water. The vertically integrated [P-Fe] (>0.22 μm fraction, [T-Fe] minus [D-Fe]) and [D-Fe] inventories throughout the water column at JB1 and JB2, where atmospheric deposition of Fe is presumably the dominant source, ranged 16,500–17,600 μmol Fe m^{-2} and 4600–4800 μmol Fe m^{-2}, respectively (Figure 3). The residence times throughout the water column were calculated to be ~1 year for [P-Fe] and 25–26 years for [D-Fe] by an estimate of Fe solubility (approximately 1%) for aerosol Fe flux (~50 μmol Fe m^{-2} d^{-1}). Particulate Fe in the deep water of Japan Sea has a very shorter residence time than [D-Fe], suggesting the rapid removal of [P-Fe] by scavenging and sinking.

[24] In our previous study [*Kitayama et al.*, 2009], the H-flu intensity levels in the North Pacific appear to increase gradually with depth in mid-depth water (~200 m to 500–1000 m depth), high in intermediate water (~500–1500 m depth), and decrease gradually with depth in deep water (~1500–5000 m depth), probably suggesting that the intermediate and deep waters in the North Pacific are originated from the North Pacific Intermediate Water (NPIW) with relatively higher H-flu intensity and the CDW with lower H-flu intensity, respectively [*Yamashita et al.*, 2007; *Yamashita and Tanoue*, 2008]. However, H-flu intensity in deep and bottom waters (below 1500–2000 m depth) of the Japan Sea is remarkably uniform with higher values (approximately 3.1–3.3) than those in the North Pacific probably because of no dominant injection of different water mass into deep and bottom waters of the Japan Sea.

[25] The depth profiles of [T-Fe] in the Japan Basin (JB1 and JB2) were remarkably similar with a mid-depth maxima at the depth of around 1500 m, then dramatically decrease with depth at the narrow depth range of 2000–2500 m and relatively uniform values in bottom water below 2500 m depth (Figures 3a and 3c). In addition, the depth profiles of water transmittance [Tr (%)] in the Japan Basin were almost same as that of water turbidity, which is contributed by the suspended particles in the water column, in a previous study [*Takata et al.*, 2008]. The lower constant [T-Fe] in bottom water than deep water was also observed at the different stations of the eastern Japan Basin in previous studies [*Takata et al.*, 2005, 2008]. These observations in bottom water were consistent in slightly higher constant [Tr (%)] and remarkably higher constant density in bottom water (Figures 3b, 3d, and 6a) and in slightly higher salinity and DO content in bottom water than the salinity and oxygen minimum layer (2000–2500 m) in deep water in the present study (Figures 6b and 6c) and in previous studies [*Gamo and Horibe*, 1983; *Gamo et al.*, 1986; *Senjyu et al.*, 2005a; *Takata et al.*, 2005]. Several studies [*Kim et al.*, 2002; *Senjyu et al.*, 2002; *Tsunogai et al.*, 2003] of bottom waters from the Japan Sea have pointed out that newly formed bottom water in the northwestern Japan Sea was observed in the summer of 2001 after the severe winter of 2000–2001. *Kim et al.* [2002] and *Senjyu et al.* [2002] reported that the new bottom water observed in the northwestern Japan Sea showed a lower temperature, higher salinity, higher DO and lower nutrient concentrations compared to the old bottom water. In addition, *Tsunogai et al.* [2003] indicated that the sharp increase in the chlorofluorocarbon (CFC) in bottom water of the northwestern Japan Sea is due to the renewal of the bottom water, which is replaced by surface water flowing down along the continental slope. A slight increase in salinity and DO concentration as well as a slight decrease in temperature and nutrient concentrations for the bottom waters provides unequivocal evidence that cold, saline, oxygen-rich and nutrient-poor surface waters were injected directly to the bottom water. Therefore, the lower uniform [T-Fe] in bottom water than those in deep water of the Japan Basin (Figure 3) are probably due to the injection of the new bottom water with the lower [T-Fe] into the Japan Basin Bottom Water (JBBW) with the anticlockwise circulation of bottom water in the Japan Basin or due to the particulate Fe removal by particle scavenging during the bottom water circulation of the Japan Basin [*Senjyu et al.*, 2005a, 2005b]. However, it is also possible that the intermediate and deep waters with the higher [T-Fe], which originated from the slope regions, injected into the Japan Basin Deep Water (JBDW).

[26] The depth profiles of [T-Fe] in the deep water column of the Yamato Basin and the slope regions were variable

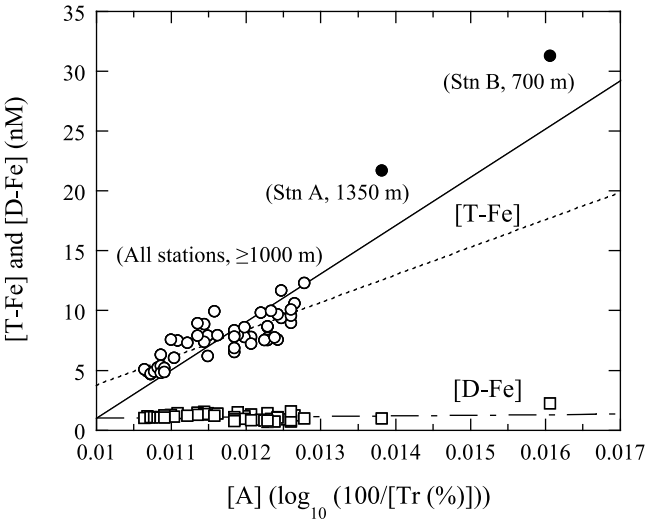

Figure 9. Total Fe concentration ([T-Fe], open and solid circles) and dissolved Fe concentration ([D-Fe], open square) versus water absorbance ([A]: $\log_{10}$ (100/[Tr (%)])) in the deep water column below 1000 m depth at all stations in addition to 700 m depth (bottom) at Station B, relatively showing linear relationships between [T-Fe] and [A] for all data (solid line) and except for 1350 m depth at Station A and 700 m depth at Station B (dotted line).

with different [T-Fe] levels among stations and were similar to those of water transmittance [Tr (%)] with the higher [T-Fe] at the lower [Tr (%)] (Figures 4 and 5). Especially, the extremely high [T-Fe] were observed in the bottom water near seafloor at Station A and B in the slope regions (Figure 5). The relative order for the [T-Fe] levels in deep and bottom waters was Station B > Station A > YB2 > YB3 = YB1 ≥ JB2 = JB1, relatively consistent with the reversed order of [Tr (%)] (Figures 3, 4, and 5). The relationship between [Tr (%)] and water absorbance ([A]) can be expressed as [A] = $\log_{10}$ (100/[Tr (%)]). Figure 9 shows the relationship between [T-Fe] below 1000 m depth at all stations in addition to 700 m depth (bottom) at Station B and [A] (solid line: [T-Fe](nM) = −39.28 + 1750.1 × [A], R = 0.8907 (n = 53)). The [P-Fe] in deep water is probably in proportion to the suspended particle concentration, which would be measured as the [Tr (%)]. In the present study, the vertical profiles of [Tr (%)] in the water column were consistent with those of the turbidity [*Takata et al.*, 2008]. The suspended particles dominantly contribute to the [Tr (%)] in the deep water column although dissolved organic matter besides suspended particles may contribute to the losses of transmittance in deep water. In addition, there are a few recent other studies for a relationship between iron concentrations and water transmission that the added iron in the surface water could be traced by the transmission profiles during the EisenEx iron fertilization experiment [*Croot et al.*, 2005] and that the large variability for iron in the mid-depth water is consistent with particle beam attenuation coefficient [*Lam and Bishop*, 2008]. Therefore, it is suggested that the high [T-Fe] and the low [Tr (%)] in the deepwater column of the Yamato Basin result from the iron supply because of the lateral transport of resuspended sediment from the continental slope. In coastal marine environments, mineral particles often represent a significant fraction of suspended particulate matter by bottom resuspension. The spectral optical properties, such as mass-specific absorption and scattering coefficients, of mineral dust suspended in seawater exhibit significantly variability associated with the origin and particle size distribution [*Stramski et al.*, 2004]. Although the [Tr (%)] at 470 nm in the present study may be influenced by the colored dissolved organic matter (CDOM) in seawater, the vertical profiles in the water column of JB1, JB2, YB2 and YB3 (Figures 3b, 3d, 4d, and 4f, respectively) were consistent with those of the turbidity in the Japan and Yamato Basins in our previous study [*Takata et al.*, 2008]. It has been reported that a large Al flux was observed in the bottom water of the Yamato Basin, probably resulting from lateral transport of particulate materials by sporadic currents [*Otosaka et al.*, 2004, 2008]. In addition, recent studies have shown that the continental margins surrounding the North Pacific provide a subsurface supply of iron that is very important to productivity [*Johnson et al.*, 1999, 2001; *Lam et al.*, 2006; *Lam and Bishop*, 2008; *Nishioka et al.*, 2007]. Thus, it may be suggested that the [T-Fe] and/or [P-Fe] could be one of the most useful chemical tracers of the physical processes in various coastal and marginal sea regions.

[27] **Acknowledgments.** We thank K. Toya, T. Nakatsuka for his technical support, and the captain and the crew of "Oshoro-Maru" of Hokkaido University for their help in the sampling. We are grateful to two anonymous reviewers for their constructive and helpful comments on this work. This work was supported by grants for the Scientific Research Project from the Research Institute for Humanity and Nature, and for the Scientific Research (18201001) from the Ministry of Education, Culture, Sports, Science and Technology.

References

Bergquist, B. A., and E. A. Boyle (2006), Dissolved iron in the tropical and subtropical Atlantic Ocean, *Global Biogeochem. Cycles*, *20*, GB1015, doi:10.1029/2005GB002505.

Bergquist, B. A., J. Wu, and E. A. Boyle (2007), Variability in oceanic dissolved iron is dominated by the colloidal fraction, *Geochim. Cosmochim. Acta*, *71*, 2960–2974, doi:10.1016/j.gca.2007.03.013.

Bruland, K. W., and E. L. Rue (2001), Analytical methods for the determination of concentrations and speciation of iron, in *The Biogeochemistry of Iron in Seawater*, edited by D. R. Turner and K. A. Hunter, pp. 255–289, John Wiley, New York.

Chase, Z., K. S. Johnson, V. A. Elrod, J. N. Plant, S. E. Fitzwater, L. Pickell, and C. M. Sakamoto (2005), Manganese and iron distributions off central California influenced by upwelling and shelf width, *Mar. Chem.*, *95*, 235–254, doi:10.1016/j.marchem.2004.09.006.

Croot, P. L., and K. A. Hunter (1998), Trace metal distributions across the continental shelf near Otago Peninsula, New Zealand, *Mar. Chem.*, *62*, 185–201, doi:10.1016/S0304-4203(98)00036-X.

Croot, P. L., P. Streu, and A. R. Baker (2004), Short residence time for iron in the surface seawater impacted by atmospheric dry deposition from Saharan dust events, *Geophys. Res. Lett.*, *31*, L23S08, doi:10.1029/2004GL020153.

Croot, P. L., et al. (2005), Spatial and temporal distribution of Fe(II) and H_2O_2 during EisenEx, an open ocean mescoscale iron enrichment, *Mar. Chem.*, *95*, 65–88, doi:10.1016/j.marchem.2004.06.041.

Croot, P. L., R. D. Frew, S. Sander, K. A. Hunter, M. J. Ellwood, S. E. Pickmere, E. R. Abraham, C. S. Law, M. J. Smith, and P. W. Boyd (2007), Physical mixing effects on iron biogeochemical cycling: FeCycle experiment, *J. Geophys. Res.*, *112*, C06015, doi:10.1029/2006JC003748.

de Baar, H. J. W., and J. T. M. de Jong (2001), Distributions, sources and sinks of iron seawater, in *The Biogeochemistry of Iron in Seawater*, edited by D. R. Tuner and K. A. Hunter, pp. 123–253, John Wiley, New York.

Duce, R. A., and N. W. Tindale (1991), Atmospheric transport of iron and its deposition in the ocean, *Limnol. Oceanogr.*, *36*, 1715–1726, doi:10.4319/lo.1991.36.8.1715.

Elrod, V. A., W. M. Berelson, K. H. Coale, and K. S. Johnson (2004), The flux of iron from continental shelf sediments: A missing source for global budgets, *Geophys. Res. Lett.*, *31*, L12307, doi:10.1029/2004GL020216.

Elrod, V. A., K. S. Johnson, S. E. Fitzwater, and J. N. Plant (2008), A long-term, high-resolution record of surface water iron concentrations in the upwelling-driven central California region, *J. Geophys. Res.*, *113*, C11021, doi:10.1029/2007JC004610.

Fitzwater, S. T., K. S. Johnson, V. A. Elrod, J. P. Ryan, L. J. Coletii, S. J. Tanner, R. M. Gordon, and F. P. Chavez (2003), Iron, nutrient and phytoplankton biomass relationships in upwelled waters of the California coastal system, *Cont. Shelf Res.*, *23*, 1523–1544, doi:10.1016/j.csr.2003.08.004.

Fung, I. Y., S. K. Meyn, I. Tegen, S. C. Doney, J. G. John, and K. B. Bishop (2000), Iron supply and demand in the upper ocean, *Global Biogeochem. Cycles*, *14*, 281–295, doi:10.1029/1999GB900059.

Gamo, T., and Y. Horibe (1983), Abyssal circulation in the Japan Sea, *J. Oceanogr.*, *39*, 220–230.

Gamo, T., Y. Nozaki, H. Sakai, T. Nakai, and H. Tsubota (1986), Spatial and temporal variations of water characteristics in the Japan Sea bottom layer, *J. Mar. Res.*, *44*, 781–793, doi:10.1357/002224086788401620.

Hansen, H. P. (1999), Determination of oxygen, in *The Methods of Seawater Analysis*, edited by K. Grasshoff, K. Kremling, and M. Ehrhardt, pp. 75–89, John Wiley-VCH, New York.

Hase, H., J.-H. Yoon, and W. Koterayama (1999), The current structure of the Tsushima Warm Current along the Japanese coast, *J. Oceanogr.*, *55*, 217–235, doi:10.1023/A:1007894030095.

Hayase, K., and N. Shinozuka (1995), Vertical distribution of fluorescent organic matter along with AOU and nutrients in the equatorial central Pacific, *Mar. Chem.*, *48*, 283–290, doi:10.1016/0304-4203(94)00051-E.

Hayase, K., H. Tsubota, I. Sunada, S. Goda, and H. Yamazaki (1988), Vertical distribution of fluorescent organic matter in the North Pacific, *Mar. Chem.*, *25*, 373–381, doi:10.1016/0304-4203(88)90117-X.

Hutchins, D. A., G. DiTullio, and K. W. Bruland (1998), An iron mosaic in the California upwelling regime, *Limnol. Oceanogr.*, *43*, 1037–1054, doi:10.4319/lo.1998.43.6.1037.

Isobe, A., M. Ando, T. Watanabe, T. Senjyu, S. Sugihara, and A. Manda (2002), Freshwater and temperature transports through the Tsushima-Korea Straits, *J. Geophys. Res.*, *107*(C7), 3065, doi:10.1029/2000JC000702.

Jickells, T. D. (1999), The inputs of dust derived elements to the Sargasso Sea: A synthesis, *Mar. Chem.*, *68*, 5–14, doi:10.1016/S0304-4203(99)00061-4.

Jickells, T. D., and L. J. Spokes (2001), Atmospheric iron inputs to the oceans, in *The Biogeochemistry of Iron in Seawater*, edited by D. R. Tuner and K. A. Hunter, pp. 85–121, John Wiley, New York.

Jo, C.-O., J.-Y. Lee, K.-A. Park, Y.-H. Kim, and K.-R. Kim (2007), Asian dust initiated early spring bloom in the northern East/Japan Sea, *Geophys. Res. Lett.*, *34*, L05602, doi:10.1029/2006GL027395.

Johnson, K. S. (2007), Developing standards for dissolved iron in seawater, *Eos Trans. AGU*, *88*(11), 131–132, doi:10.1029/2007EO110003.

Johnson, K. S., R. M. Gordon, and K. H. Coale (1997), What controls dissolved iron concentrations in the world ocean?, *Mar. Chem.*, *57*, 137–161, doi:10.1016/S0304-4203(97)00043-1.

Johnson, K. S., F. P. Chavez, and G. E. Friederich (1999), Continental-shelf sediment as a primary source of iron for coastal phytoplankton, *Nature*, *398*, 697–700, doi:10.1038/19511.

Johnson, K. S., F. P. Chavez, V. A. Elrod, S. E. Fitzwater, J. T. Pennington, K. R. Buck, and P. M. Waltz (2001), The annual cycle of iron and the biological response in central California waters, *Geophys. Res. Lett.*, *28*, 1247–1250, doi:10.1029/2000GL012433.

Kim, K.-R., G. Kim, and K. Kim (2002), A sudden bottom-water formation during the severe winter 2000–2001: The case of the East/Japan Sea, *Geophys. Res. Lett.*, *29*(8), 1234, doi:10.1029/2001GL014498.

Kitayama, S., et al. (2009), Controls on iron distributions in the deep water column of the North Pacific Ocean: Iron(III) hydroxide solubility and marine humic-type dissolved organic matter, *J. Geophys. Res.*, *114*, C08019, doi:10.1029/2008JC004754.

Kuma, K., J. Nishioka, and K. Matsunaga (1996), Controls on iron(III) hydroxide solubility in seawater: The influence of pH and natural organic chelators, *Limnol. Oceanogr.*, *41*, 396–407, doi:10.4319/lo.1996.41.3.0396.

Kuma, K., A. Katsumoto, N. Shiga, T. Sawabe, and K. Matsunaga (2000), Variation of size-fractionated Fe concentrations and Fe(III) hydroxide solubilities during a spring phytoplankton bloom in Funka Bay (Japan), *Mar. Chem.*, *71*, 111–123, doi:10.1016/S0304-4203(00)00044-X.

Kuma, K., Y. Isoda, and S. Nakabayashi (2003), Control on dissolved iron concentrations in deep waters in the western North Pacific: Iron(III) hydroxide solubility, *J. Geophys. Res.*, *108*(C9), 3289, doi:10.1029/2002JC001481.

Kumamoto, Y., T. Aramaki, S. Watanabe, M. Yoneda, Y. Shibata, O. Togawa, M. Morita, and K. Shitashima (2008), Temporal and spatial variations of radiocarbon in Japan Sea bottom water, *J. Oceanogr.*, *64*, 429–441, doi:10.1007/s10872-008-0036-y.

Laës, A., S. Blain, P. Laan, E. P. Achterberg, G. Sarthou, and H. J. W. de Baar (2003), Deep dissolved iron profiles in the eastern North Atlantic in relation to water masses, *Geophys. Res. Lett.*, *30*(17), 1902, doi:10.1029/2003GL017902.

Laës, A., S. Blain, P. Laan, S. J. Ussher, E. P. Achterberg, P. Treguer, and H. J. W. de Baar (2007), Sources and transport of dissolved iron and manganese along the continental margin of the Bay of Biscay, *Biogeosciences*, *4*, 181–194, doi:10.5194/bg-4-181-2007.

Laglera, L. M., and C. M. G. van den Berg (2009), Evidence for geochemical control of iron by humic substances in seawater, *Limnol. Oceanogr.*, *54*, 610–619.

Lam, P. J., and J. K. B. Bishop (2008), The continental margin is a key source of iron to the HNLC North Pacific Ocean, *Geophys. Res. Lett.*, *35*, L07608, doi:10.1029/2008GL033294.

Lam, P. J., J. K. B. Bishop, C. C. Henning, M. A. Marcus, G. A. Waychunas, and I. Y. Fung (2006), Wintertime phytoplankton bloom in the subarctic Pacific supported by continental margin iron, *Global Biogeochem. Cycles*, *20*, GB1006, doi:10.1029/2005GB002557.

Lohan, M. C., A. M. Aguilar-Islas, R. P. Franks, and K. W. Bruland (2005), Determination of iron and copper in the seawater at pH 1.7 with a new commercially available chelating resin, NTA Superflow, *Anal. Chim. Acta*, *530*, 121–129, doi:10.1016/j.aca.2004.09.005.

Mahowald, N. M., A. R. Baker, G. Bergametti, N. Brooks, R. A. Duce, T. D. Jickells, N. Kubilay, J. M. Prospero, and I. Tegen (2005), Atmospheric global dust cycle and iron inputs to the ocean, *Global Biogeochem. Cycles*, *19*, GB4025, doi:10.1029/2004GB002402.

Martin, J. H., and R. M. Gordon (1988), Northeast Pacific iron distributions in relation to phytoplankton productivity, *Deep Sea Res.*, *35*, 177–196, doi:10.1016/0198-0149(88)90035-0.

Martin, J. H., R. M. Gordon, S. Fitzwater, and W. W. Broenkow (1989), VERTEX: Phytoplankton/iron studies in the Gulf of Alaska, *Deep Sea Res.*, *36*, 649–680, doi:10.1016/0198-0149(89)90144-1.

Mopper, K., and C. A. Schultz (1993), Fluorescence as a possible tool for studying the nature and water column distribution of DOC components, *Mar. Chem.*, *41*, 229–238, doi:10.1016/0304-4203(93)90124-7.

Nakabayashi, S., M. Kusakabe, K. Kuma, and I. Kudo (2001), Vertical distributions of iron(III) hydroxide solubility and dissolved iron in the northwestern North Pacific Ocean, *Geophys. Res. Lett.*, *28*, 4611–4614, doi:10.1029/2001GL013591.

Nishioka, J., S. Takeda, I. Kudo, D. Tsumune, T. Yoshimura, K. Kuma, and A. Tsuda (2003), Size-fractionated iron distributions and iron-limitation processes in the subarctic NW Pacific, *Geophys. Res. Lett.*, *30*(14), 1730, doi:10.1029/2002GL016853.

Nishioka, J., et al. (2007), Iron supply to the western subarctic Pacific: Importance of iron export from the Sea of Okhotsk, *J. Geophys. Res.*, *112*, C10012, doi:10.1029/2006JC004055.

Obata, H., H. Karatani, and E. Nakayama (1993), Automated determination of iron in seawater by chelating resin concentration and chemiluminescence detection, *Anal. Chem.*, *65*, 1524–1528, doi:10.1021/ac00059a007.

Obata, H., D. S. Alibo, and Y. Nozaki (2007), Dissolved aluminum, indium, and cerium in the Sea of Japan and the Sea of Okhotsk: Comparison to the marginal seas of the western North Pacific, *J. Geophys. Res.*, *112*, C12003, doi:10.1029/2006JC003944.

Ooki, A., J. Nishioka, T. Ono, and S. Noriki (2009), Size dependence of iron solubility of Asian mineral dust particles, *J. Geophys. Res.*, *114*, D03202, doi:10.1029/2008JD010804.

Otosaka, S., O. Togawa, M. Baba, E. Karasev, Y. N. Volkov, N. Omata, and S. Noriki (2004), Lithogenic flux in the Japan Sea measured with sediment traps, *Mar. Chem.*, *91*, 143–163, doi:10.1016/j.marchem.2004.06.006.

Otosaka, S., T. Tanaka, O. Togawa, H. Amano, E. V. Karasev, M. Minakawa, and S. Noriki (2008), Deep sea circulation of particulate organic carbon in the Japan Sea, *J. Oceanogr.*, *64*, 911–923, doi:10.1007/s10872-008-0075-4.

Saitoh, Y., K. Kuma, Y. Isoda, H. Kuroda, H. Matsuura, T. Wagawa, H. Takata, N. Kobayashi, S. Nagao, and T. Nakatsuka (2008), Processes influencing iron distribution in the coastal water of the Stugaru Strait, Japan, *J. Oceanogr.*, *64*, 815–830, doi:10.1007/s10872-008-0068-3.

Schlosser, C., and P. L. Croot (2009), Controls on seawater Fe(III) solubility in the Mauritanian upwelling zone, *Geophys. Res. Lett.*, *36*, L18606, doi:10.1029/2009GL038963.

Senjyu, T., and H. Sudo (1993), Water characteristics and circulation of the upper portion of the Japan Sea proper water, *J. Mar. Syst.*, *4*, 349–362, doi:10.1016/0924-7963(93)90029-L.

Senjyu, T., and H. Sudo (1994), The upper portion of the Japan Sea proper water; its source and circulation as deduced from isopycnal analysis, *J. Oceanogr.*, *50*, 663–690, doi:10.1007/BF02270499.

Senjyu, T., T. Aramaki, S. Otosaka, O. Togawa, M. Danchenkov, E. Karasev, and Y. Volkov (2002), Renewal of the bottom water after the winter 2000–2001 may spin up the thermohaline circulation in the Japan Sea, *Geophys. Res. Lett.*, *29*(7), 1149, doi:10.1029/2001GL014093.

Senjyu, T., Y. Isoda, T. Aramaki, S. Otosaka, S. Fujio, D. Yanagimoto, T. Suzuki, K. Kuma, and K. Mori (2005a), Benthic front and the Yamato Basin bottom water in the Japan Sea, *J. Oceanogr.*, *61*, 1047–1058, doi:10.1007/s10872-006-0021-2.

Senjyu, T., H.-R. Shin, J.-H. Yoon, Z. Nagano, H.-S. An, S.-K. Byun, and C.-K. Lee (2005b), Deep flow field in the Japan/East Sea as deduced from direct current measurements, *Deep Sea Res., Part II*, *52*, 1726–1741, doi:10.1016/j.dsr2.2003.10.013.

Stramski, D., S. B. Wozniak, and P. J. Flatau (2004), Optical properties of Asian mineral dust suspended in seawater, *Limnol. Oceanogr.*, *49*, 749–755, doi:10.4319/lo.2004.49.3.0749.

Sudo, H. (1986), A note on the Japan Sea proper water, *Prog. Oceanogr.*, *17*, 313–336, doi:10.1016/0079-6611(86)90052-2.

Suzuki, R., and T. Ishimaru (1990), An improved method for the determination of phytoplankton chlorophyll using N, N-dimethylformamide, *J. Oceanogr.*, *46*, 190–194.

Takata, H., et al. (2004), Spatial variability of iron in the surface water of the northwestern North Pacific Ocean, *Mar. Chem.*, *86*, 139–157, doi:10.1016/j.marchem.2003.12.007.

Takata, H., K. Kuma, S. Iwade, Y. Isoda, H. Kuroda, and T. Senjyu (2005), Comparative vertical distributions of iron in the Japan Sea, the Bering Sea and the western North Pacific Ocean, *J. Geophys. Res.*, *110*, C07004, doi:10.1029/2004JC002783.

Takata, H., K. Kuma, Y. Saitoh, M. Chikira, S. Saitoh, Y. Isoda, S. Takagi, and K. Sakaoka (2006), Comparing the vertical distribution of iron in the eastern and western North Pacific Ocean, *Geophys. Res. Lett.*, *33*, L02613, doi:10.1029/2005GL024538.

Takata, H., K. Kuma, Y. Isoda, S. Otosaka, T. Senjyu, and M. Minagawa (2008), Iron in the Japan Sea and its implications for the physical processes in deep water, *Geophys. Res. Lett.*, *35*, L02606, doi:10.1029/2007GL031794.

Talley, L. D. (1995), Some advances in understanding of the general circulation of the Pacific Ocean, with emphasis on recent U.S. contributions, *Rev. Geophys.*, *33*, 1335–1352, doi:10.1029/95RG00350.

Tani, H., J. Nishioka, K. Kuma, H. Takata, Y. Yamashita, E. Tanoue, and T. Midorikawa (2003), Iron(III) hydroxide solubility and humic-type fluorescent organic matter in the deep water column of the Okhotsk Sea and the northwestern North Pacific Ocean, *Deep Sea Res., Part I*, *50*, 1063–1078, doi:10.1016/S0967-0637(03)00098-0.

Tsunogai, S., K. Kawada, S. Watanabe, and T. Aramaki (2003), CFC indicating renewal of the Japan Sea deep water in winter 2000–2001, *J. Oceanogr.*, *59*, 685–693, doi:10.1023/B:JOCE.0000009597.33460.d7.

Uematsu, M., Z. Wang, and I. Uno (2003), Atmospheric input of mineral dust to the western North Pacific region based on direct measurements and a regional chemical transport model, *Geophys. Res. Lett.*, *30*(6), 1342, doi:10.1029/2002GL016645.

Ussher, S. J., P. J. Worsfold, E. P. Achterberg, A. Laës, S. Blain, P. Laan, and H. J. W. de Baar (2007), Distributions and redox speciation of dissolved iron on the European continental margin, *Limnol. Oceanogr.*, *52*, 2530–2539.

Watanabe, T., O. Katoh, and H. Yamada (2006), Structure of the Tsushima Warm Current in the northeastern Japan Sea, *J. Oceanogr.*, *62*, 527–538, doi:10.1007/s10872-006-0073-3.

Yamashita, Y., and E. Tanoue (2008), Production of bio-refractory fluorescent dissolved organic matter in the ocean interior, *Nat. Geosci.*, doi:10.1038/ngeo279.

Yamashita, Y., A. Tsukasaki, T. Nishida, and E. Tanoue (2007), Vertical and horizontal distribution of fluorescent dissolved organic matter in the Southern Ocean, *Mar. Chem.*, *106*, 498–509, doi:10.1016/j.marchem.2007.05.004.

T. Aramaki, Environmental Chemistry Division, National Institute for Environmental Studies, 16-2 Onogawa, Tsukuba, Ibaraki 305-8506, Japan.

S. Fujita, K. Kuma, S. Ishikawa, Y. Nakayama, S. Nishimura, and S. Ushizaka, Graduate School of Environmental Science, Hokkaido University, Kita 10-Nishi 5, Kita-ku, Sapporo, Hokkaido 060-0810, Japan. (kuma@fish.hokudai.ac.jp)

Y. Isoda, Faculty of Fisheries Sciences, Hokkaido University, 3-1-1 Minato, Hakodate, Hokkaido 041-8611, Japan.

S. Otosaka, Research Group for Environmental Science, Japan Atomic Energy Agency, Naka-gun, Ibaraki 319-1195, Japan.